Journal of Power Sources, *30* (1990) 77 - 97

PROCESSES AT THE MICRO-LEVEL IN THE OXIDATION OF $PbSO_4$ TO PbO_2 DURING CHARGING OF LEAD/ACID BATTERY POSITIVE PLATES

D. PAVLOV* and E. BASHTAVELOVA

Central Laboratory of Electrochemical Power Sources, Bulgarian Academy of Sciences, 1040 Sofia (Bulgaria)

D. SIMONSSON and P. EKDUNGE

Royal Institute of Technology, Stockholm (Sweden)

Introduction

The structure of the positive active mass is developed during lead/acid battery plate manufacture [1, 2]. The crystals of the paste are oxidized to PbO_2 through electrochemical processes. Formation of the PbO_2 active mass proceeds mainly by metasomatic processes [3] whereby the crystals of basic lead sulphates, lead oxide, and lead sulphate are transformed into microporous agglomerates of small PbO_2 particles [1]. These agglomerates are inter-connected in a macroporous skeleton that mechanically supports the active mass and conducts the electric current. Part of the skeleton disintegrates during discharge and is then rebuilt during the next battery charge. The active mass undergoes hundreds of such cycles; this suggests that one and the same structure is maintained. What are the reasons for this reversibility and stability of the structure despite the considerable alteration to which the active material is subjected during each cycle? It might be supposed that during charge the newly-formed active mass reproduces the structural disposition of the unreacted PbO_2. This could happen if the crystallization processes taking place during charge are similar to those occurring during plate formation.

The aim of this paper is to describe qualitatively the elementary processes taking place during charge, as well as to assess their influence on the structure of the active mass.

Experimental

Morphological and structural investigations

Scanning electron microscopy (SEM) was used to study the crystallization processes at the micro-level (from 0.1 to several microns). SEM

*Author to whom correspondence should be addressed.

0378-7753/90/$3.50

observations of the morphology of the crystals and particles, as well as the structure of the active mass, were the main experimental methods used in this work.

Determination of lead-ion concentration in the plate pores

Lead ions are part of the solid initial and final products of the charge reaction. Hence, the ions are involved in some elementary processes occurring in the solution contained in the pores of the active mass. It was therefore necessary to determine the concentration of these ions in the pores during charge. A special cell was designed for this purpose. Its general design is presented in Fig. 1. The cell contained one negative and one positive plate that formed the two opposite walls of the cell. The frame of the positive plate was sealed to the cell wall by epoxy resin so that the solution could flow through the plate pores only. By exerting pressure on the solution in the cell, a certain volume of it passes through the pores, carrying away the dissolved lead ions and complexes. This solution was filtered through the separator ($r < 0.5\ \mu m$) and collected in a flask. After dilution of the sample, the total lead ion concentration (Pb^{2+}, Pb^{4+}, soluble lead hydroxides) was determined by atomic absorption spectrometry (AAS).

To carry out these functions, the cell was closed and connected to a pump and a vessel containing H_2SO_4 solution (sp. gr. 1.28). The solution was pumped into the cell at a rate of 1 ml min^{-1}. The positive plate potential was measured *versus* an Hg/Hg_2SO_4 reference electrode.

Electrodes

Positive plate grids (3 × 4 cm) were cast from a lead alloy containing 6 wt.% Sb, 0.1 wt.% As, and 0.1 wt.% Sn. The paste was prepared at 30 °C from a mixture of leady oxide (65% degree of oxidation) and H_2SO_4 solution

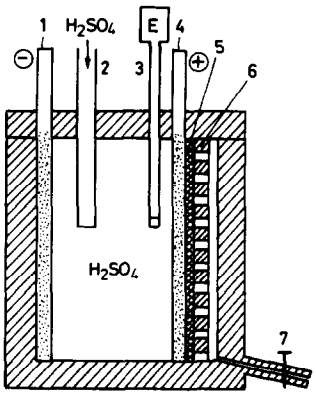

Fig. 1. Cell for determining lead ion concentration. 1, Negative plate; 2, inlet tube for H_2SO_4 addition; 3, Hg/Hg_2SO_4 reference electrode; 4, positive plate; 5, sheet of microporous separator; 6, perforated supporting plate; 7, collection point for H_2SO_4 solution containing lead ions.

(sp. gr. 1.4) in an H_2SO_4/PbO ratio equal to 4.5%. Each plate was pasted to a density of 4.2 g cm^{-3}. After curing and formation by classical manufacturing methods, the plates were assembled in cells that each contained one positive and two negative plates, and H_2SO_4 solution (sp. gr. 1.28). The cells were subjected to five 'conditioning' cycles (3 h discharge to 80% DOD; 9 h charge with 15% overcharge), and then charge/discharge test studies were conducted. Samples for SEM observations were taken from fully discharged cells, and from plates with an increasing state-of-charge, *i.e.*, $Q_{charge}/Q_{discharge} = 50$, 80, and 100%.

Part of each sample was treated with a solution of H_2O_2 and HNO_3, whereupon the PbO_2 particles dissolved and the structure of the remaining $PbSO_4$ crystallites was observed.

Results

Discharged positive plates

As established earlier [2], during discharge and at open circuit thereafter, some of the $PbSO_4$ crystals formed during the process

$$PbO_2 + H_2SO_4 + 2H^+ + 2e^- \longrightarrow (PbSO_4)^0 + 2H_2O \quad (1)$$

can recrystallize

$$(PbSO_4)^0 \longrightarrow (PbSO_4)^{cr} \quad (2)$$

This stage is associated with the formation of $PbSO_4$ crystallites with well-shaped walls, edges, and apices.

Micrographs of the active mass discharged at 2 mA cm^{-2} are presented in Fig. 2. Figure 2(a) shows that $PbSO_4$ crystals (the large, smooth regions) are shapeless and connected to the PbO_2 skeleton. The small grains are PbO_2 particles. There are few pores with a small cross section. Hence, the access of fresh H_2SO_4 solution from the exterior electrolyte has decreased considerably. Figure 2(b) shows another part of the discharged active mass from the same plate. In the large pores, $PbSO_4$ crystals with well-shaped walls, edges, and apices are formed. Hence, $PbSO_4$ crystallization and/or recrystallization takes place in the macropores where the access of fresh H_2SO_4 solution is facilitated.

To determine the mechanism by which $PbSO_4$ is bound to the PbO_2 skeleton, pieces of the active mass were glued with epoxy resin, polished, and subjected to SEM observation. The respective micrographs are given in Fig. 3(a) and (b). The fine grains and needles consist of unreacted PbO_2 particles. They are bound together in microporous agglomerates of larger or smaller size. The large, smooth areas represent the cross section of the $PbSO_4$ crystals. The latter form a shapeless mass with small pores usually surrounded by PbO_2 particles (circle a). The $PbSO_4$ also forms well-shaped crystals (circle b), usually in the large pores. It is noticed that some shapeless $PbSO_4$ crystals incorporate groups of PbO_2 particles (or agglomerates) and even pores (circle c).

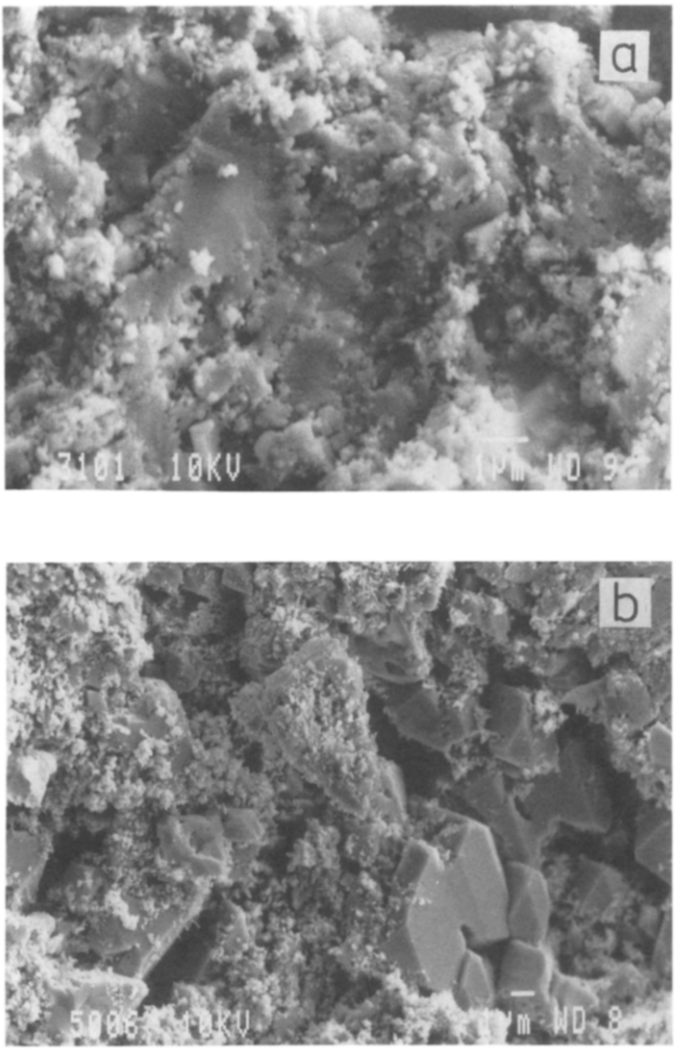

Fig. 2. Electron micrographs of discharged active mass. Discharge current density: 2 mA cm^{-2}. Magnification bar = 1 μm.

$PbSO_4$ crystals of better definition were observed after dissolution of the residual PbO_2 (Fig. 4(a, b)). It can be seen that many of the $PbSO_4$ crystals have cavities formed after the dissolution of PbO_2. Many rounded crystals are also observed. They have probably been encircled by the PbO_2 skeleton. Only those $PbSO_4$ crystals in the vicinity of macropores have well-shaped walls, edges, and apices.

The recrystallization process is even more clearly expressed when the discharged plate is stored at open circuit in H_2SO_4 solution for 30 - 100 h (Fig. 5). Under these conditions, large, well-shaped $PbSO_4$ crystals are formed and the PbO_2 skeleton can be distinguished easily from the $PbSO_4$ crystals. It is

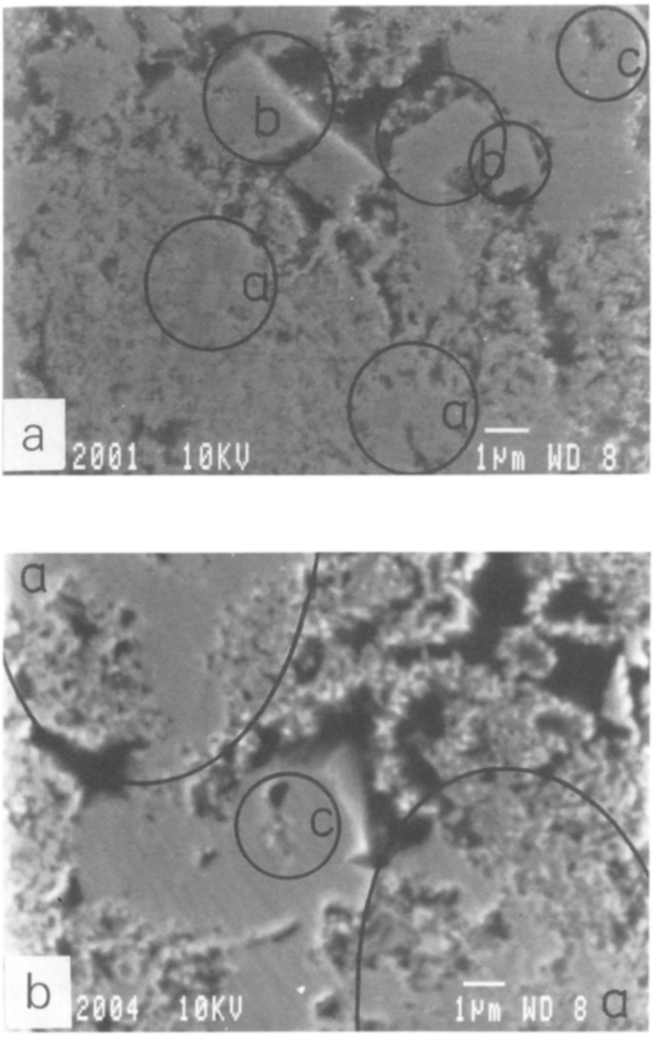

Fig. 3. Electron micrographs of discharged active mass at 20 mA cm^{-2}. Active mass polished along cross section of plate. Magnification bar = 1 μm.

obvious, therefore, that a process of rearrangement of the $PbSO_4$ crystals and the PbO_2 skeleton takes place at open circuit.

Appearance of active mass during charge

Mechanism of PbO_2 agglomerate growth

Two regimes of charge were employed: galvanostatic at 7.0 or 13.3 mA cm^{-2}, and potentiostatic at overvoltages of 100 or 250 mV to 50% and 80% state-of-charge. Micrographs of the active mass are presented in Fig. 6.

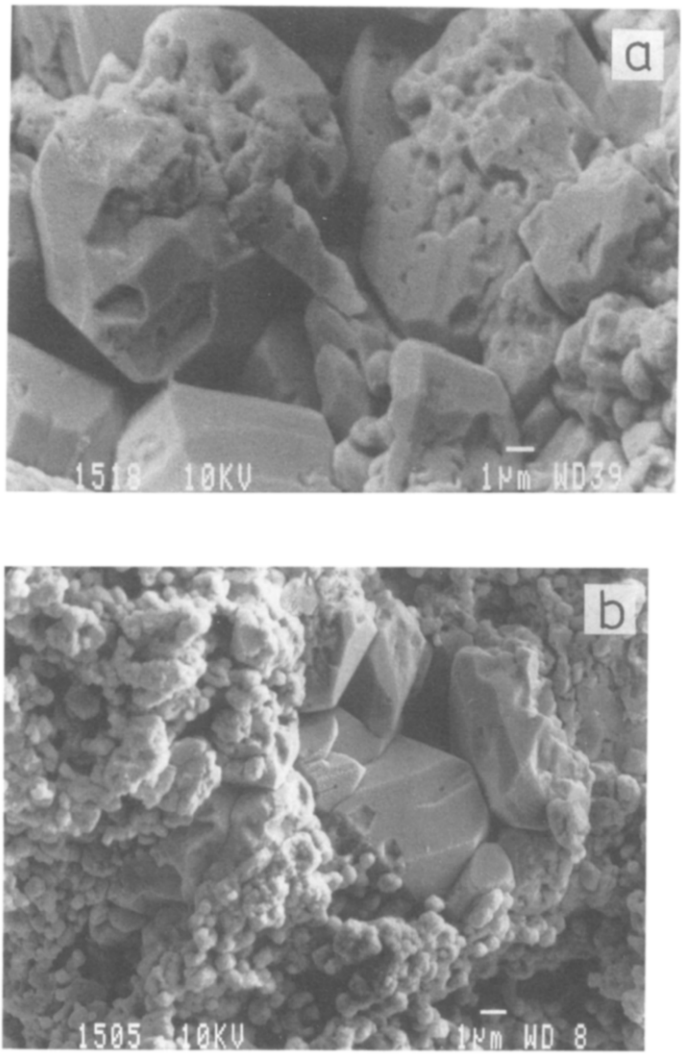

Fig. 4. Electron micrographs of $PbSO_4$ crystals in discharged active mass (PbO_2 agglomerates dissolved in H_2O_2). Discharge current density: 2 mA cm^{-2}. Magnification bar = 1 μm.

Partially oxidized $PbSO_4$ crystals were chosen in this case. Two mechanisms for the formation of PbO_2 agglomerates are revealed by the above pictures:

(i) Metasomatic mechanism (see circled region in Fig. 6(b) and (c)). PbO_2 agglomerates are formed in the matrix of the $PbSO_4$ crystals. This mechanism has been described previously [4 - 6]. The oxidized $PbSO_4$ crystal is closely connected to the PbO_2 skeleton, whereby the latter leads away the electrons generated by the electrochemical reaction. The newly-formed PbO_2 particles of the growing agglomerate are a mechanical and electrical continuation of

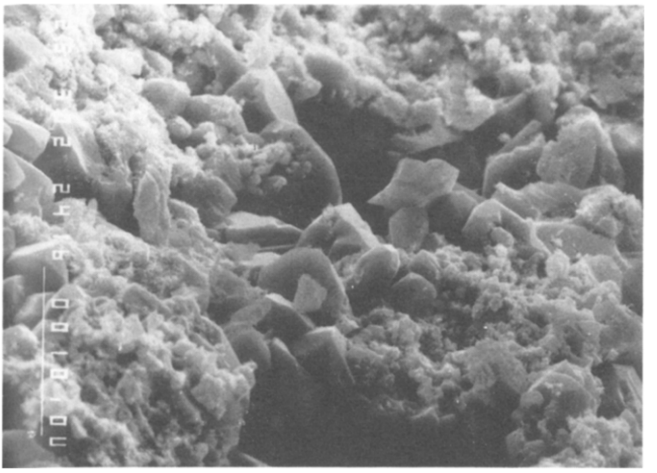

Fig. 5. Electron micrograph of discharged active mass after storage in H_2SO_4 for 48 h. Recrystallization process of $PbSO_4$ in advanced stage. Magnification bar = 10 μm.

the PbO_2 skeleton. The newly-formed PbO_2 agglomerate advances into the interior of the $PbSO_4$ crystal. Since the PbO_2 molar volume is much smaller than that of $PbSO_4$, micropores will be formed in the agglomerate. Free access of H^+, HSO_4^- and SO_4^{2-} ions, and H_2O should be permitted from the bulk of the electrolyte to the reaction layer between the oxidized crystal and the newly-formed PbO_2 agglomerate.

(ii) Free formation of PbO_2 agglomerates (Fig. 6(a)). In this case, PbO_2 agglomerates are formed outside the matrix of $PbSO_4$ crystals. This phenomenon can be observed when the dissolution rate of $PbSO_4$ crystals and the diffusion rate of Pb^{2+} ions are significantly larger than the rate of nucleation and growth of PbO_2 particles. Under these conditions, Pb^{2+} ions leave the volume of the $PbSO_4$ crystal being dissolved, pass into the pores, and reach the PbO_2 agglomerates that are in electronic contact with the PbO_2 skeleton. An electrochemical reaction proceeds at the surface of the agglomerates.

Oxidation via either of the two mechanisms takes place simultaneously at different sites on the plate. These mechanisms can even be observed in neighbouring regions of the same $PbSO_4$ crystal.

Morphology of the PbO_2 particles

The shape of the newly formed PbO_2 particles was examined. The plates were charged potentiostatically (at 100 or 250 mV). Figure 7(a) presents a portion of the $PbSO_4$ crystal where oxidation has just commenced. It can be seen that PbO_2 particles are needle-like in shape with a diameter of 0.06 - 0.08 μm, and a length of 0.1 - 0.4 μm. Takehara and Kanamura [6] have established that the size of PbO_2 crystals depends on the concentration of the

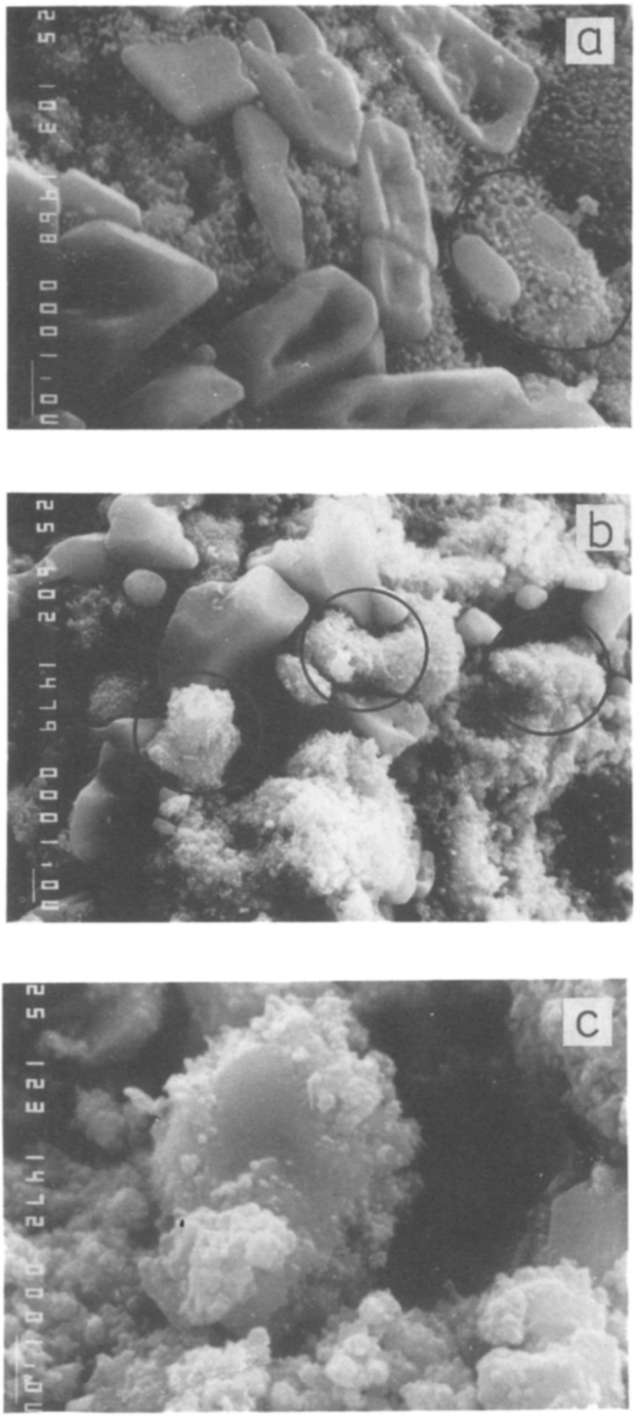

Fig. 6. Electron micrographs of active mass at 50% state-of-charge. Current density: 13.3 mA cm^{-2}. Magnification bar = 1 μm.

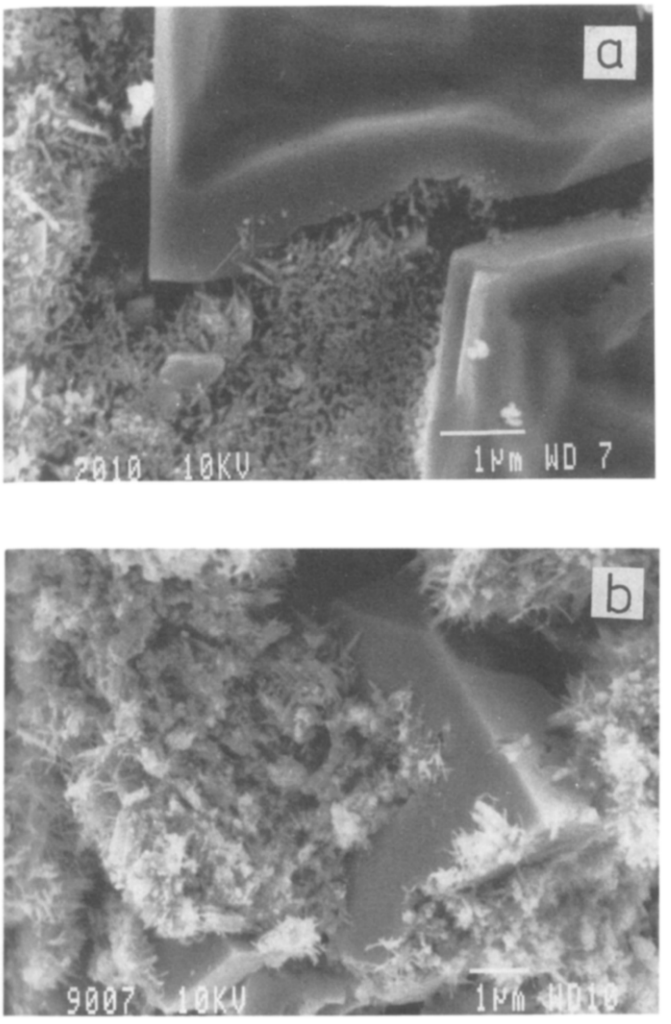

Fig. 7. Electron micrographs of active mass at 50% state-of-charge. (a) Overvoltage 100 mV; (b) overvoltage 250 mV. Newly formed PbO_2 particles are dendritic. Magnification bar = 1 μm.

H_2SO_4 solution, namely, the size decreases with increase in H_2SO_4 concentration. As seen from the micrograph in Fig. 7(b), some PbO_2 crystals grow at the site of contact with $PbSO_4$ crystals. Others grow as dendrites in the pore volume. Branched dendrites are also observed (Fig. 7(b)). $PbSO_4$ crystal oxidation occurs at preferred sites.

The newly formed PbO_2 particles can also take the form of grains (Fig. 8). PbO_2 grains differ in size and are inter-connected in either circular agglomerates or in chains. There is a complex inter-relation between the processes occurring at a given site of the dissolving $PbSO_4$ crystal and the growing PbO_2 particle.

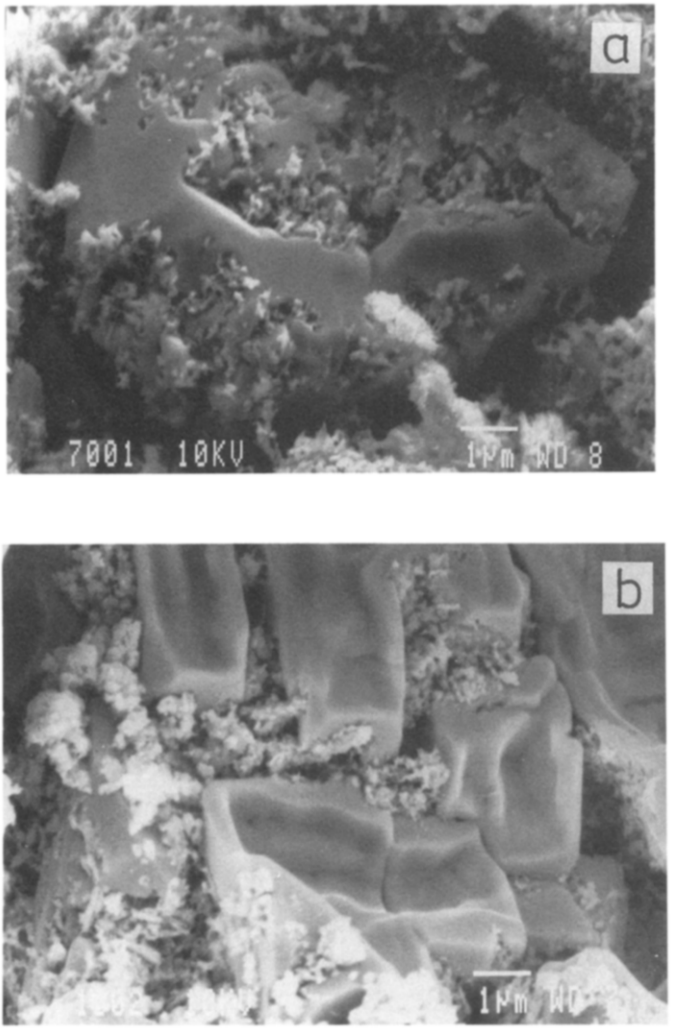

Fig. 8. Electron micrographs of active mass at 50% state-of-charge. Overvoltage 250 mV. Newly formed PbO_2 particles are granular. Magnification bar = 1 μm.

The micrograph in Fig. 9 demonstrates the progress of the oxidation process from one $PbSO_4$ crystal to the next. The mechanism of PbO_2 agglomerate formation is a metasomatic one. Both needle-like and grain-shaped PbO_2 particles are observed. This implies that their nucleation depends on the conditions in a very small pore volume where the reactions proceed.

According to the theory of crystal growth, crystal apices are, energetically, the richest parts of the crystal; hence they dissolve most readily, while edges and walls are less susceptible to dissolution. This implies that, during oxidation, $PbSO_4$ crystals will become rounded and will form spherical particles. This mechanism is observed with many of the $PbSO_4$ crystals shown

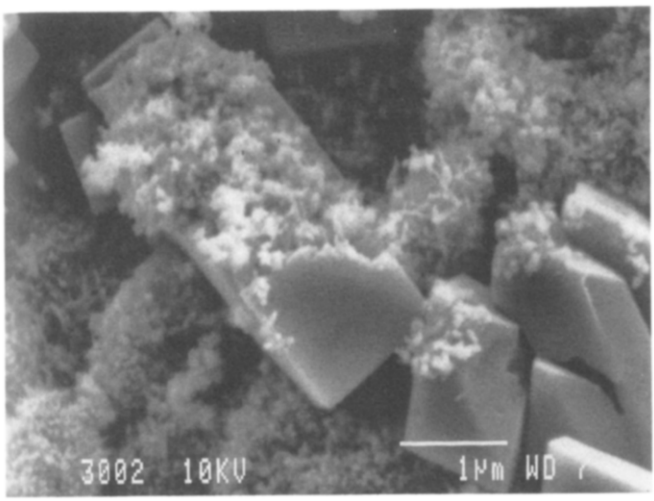

Fig. 9. Electron micrograph of active mass at 80% state-of-charge and 250 mV overvoltage. Oxidation process progresses from one crystal to the next, then within the $PbSO_4$ crystal. Metasomatically formed PbO_2 agglomerates also observed. Magnification bar = 1 μm.

in Figs. 6 and 8. On the other hand, Figs. 7 and 9 show $PbSO_4$ crystals with well-expressed apices and edges, in spite of the fact that portions of these $PbSO_4$ crystals are oxidized to PbO_2. This implies that the Pb^{2+}-ion concentration in the vicinity of the $PbSO_4$ crystal is maintained at a lower value than that corresponding to the $PbSO_4$ solubility. The apices and edges of the crystal are unaffected by this lower concentration. This can occur when these parts of the $PbSO_4$ crystal are passivated or their dissolution is strongly inhibited. Most probably, a definite ratio between passivated and non-passivated parts of the $PbSO_4$ crystals exists in the active mass; this will affect the charge efficiency. The larger the amount of passivated $PbSO_4$ crystals (or parts of them) the stronger will be the electrode polarization and, hence, the lower the charging efficiency.

In order to reveal the progress of the oxidation process in the $PbSO_4$ matrix, portions of the active material were treated with H_2O_2. Figure 10(a) and (b) shows the remaining unoxidized portions of the $PbSO_4$ crystals at two magnifications. Two types of $PbSO_4$ crystals are visible: the first comprises large, and sometimes well-shaped, crystals; the second comprises small remnants of the unoxidized portions. This is a clear illustration of the progress of the metasomatic process inside the bulk of the crystal. Some regions of the crystal interior are dissolved faster than the rest, whereby small grains are formed (Fig. 10). This non-homogeneity is most likely due to structural defects caused by foreign ions and surfactants included in the bulk of the $PbSO_4$ crystal. Residual PbO_2 particles included in the $PbSO_4$ crystal during discharge may play a certain role, too. The irregular oxidation of $PbSO_4$ crystals might also depend on some transport hindrances of H^+, HSO_4^- and SO_4^{2-}, and H_2O to each micro-volume of the reaction layer.

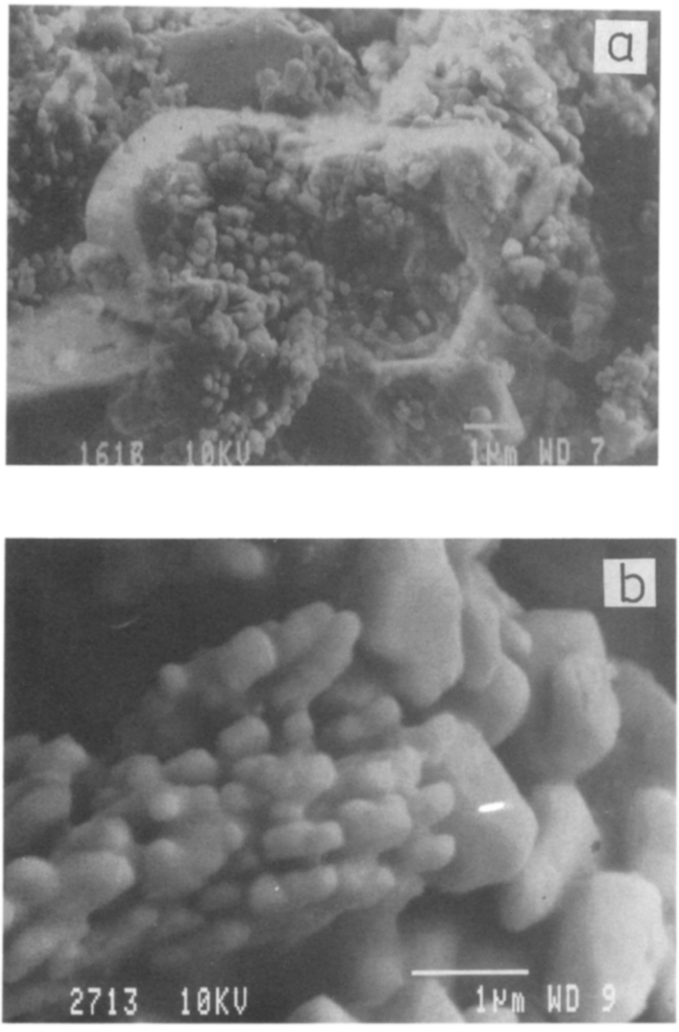

Fig. 10. Electron micrographs of $PbSO_4$ crystals of active mass at 80% state-of-charge. (PbO_2 skeleton dissolved in H_2O_2.) Overvoltage 100 mV. Oxidation process proceeds by metasomatic mechanism and has advanced into interior of $PbSO_4$ crystal. Grains of unoxidized $PbSO_4$ also present. Magnification bar = 1 μm.

Charged active mass

SEM micrographs of samples taken from the active mass at 100% state-of-charge are presented in Fig. 11. Well-formed, microporous PbO_2 agglomerates are inter-connected into a skeleton containing micropores. Both needle-like and granular PbO_2 particles can be seen.

Portions of the active mass were treated with H_2O_2. Figure 12 shows the remaining unoxidized $PbSO_4$ crystals at 100% state-of-charge. A large number of small, rounded $PbSO_4$ crystallites are visible; these have probably remained unoxidized in the interior of the PbO_2 agglomerates. Only a few,

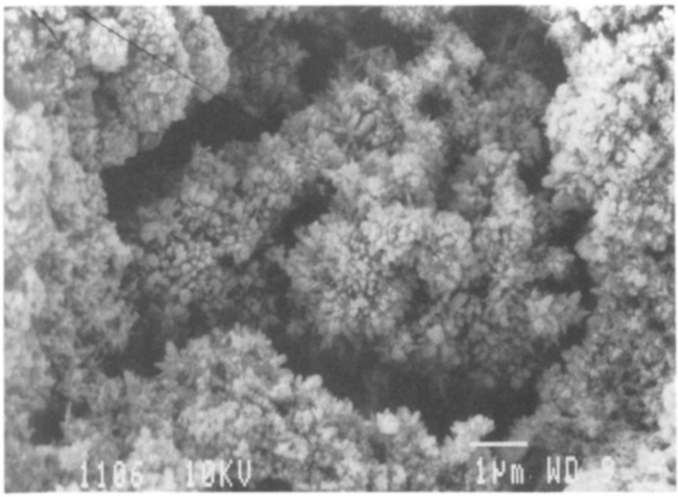

Fig. 11. Electron micrograph of active mass at 100% state-of-charge. Overvoltage 100 mV. Black regions are macropores. Magnification bar = 1 μm.

large $PbSO_4$ crystals are observed; these have been passivated. Some of the latter crystals even have well-shaped apices and edges.

Lead-ion concentration in the active mass pores

After five conditioning cycles, the charged plate was washed, dried, and inserted in a cell that was used for determining the lead-ion concentration in

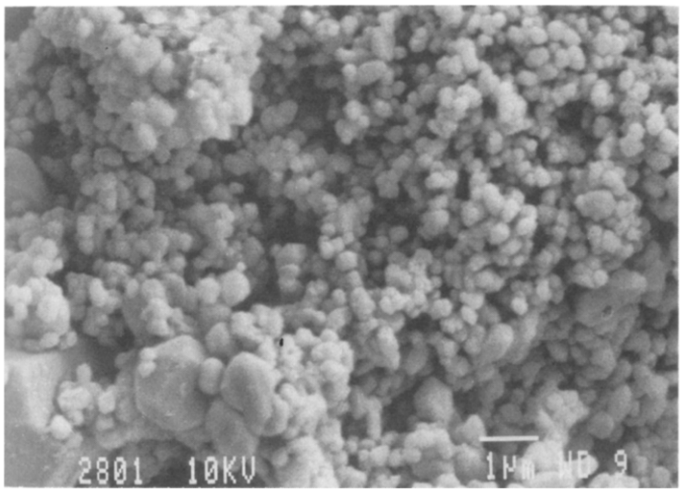

Fig. 12. Electron micrograph of $PbSO_4$ crystals remaining after treatment of charged active mass with H_2O_2. Overvoltage 250 mV. Small $PbSO_4$ grains are incorporated in PbO_2 agglomerates and thus remain unoxidized. Magnification bar = 1 μm.

the pores of the active mass (Fig. 1). Two additional cycles were carried out: 4 h charge at 15 mA cm^{-2} and 5 h discharge at 13.3 mA cm^{-2}. The cell was then left on open circuit for 2 h, and subsequently discharged.

Discharge

Figure 13 presents the results of the discharge experiments (4 h at 15 mA cm^{-2}). $PbSO_4$ solubility in H_2SO_4 (sp. gr. 1.28), measured in mg l^{-1}, is given in Table 1. These solubility values are marked on the right-hand side of Fig. 13. It is seen that by the end of discharge the concentration of the soluble Pb-ion species in the pores of the active mass corresponds to the solubility of $PbSO_4$. A most characteristic feature of these curves is the appearance of a maximum at the beginning of discharge. Such a maximum has been observed by Takehara and Kanamura [11], and by Hameenoja *et al.* [12] in their study of the reduction of PbO_2 by means of rotating disc electrodes. This maximum could be related to the low nucleation rate of $PbSO_4$. Nucleation can start only above a certain supersaturation. Another reason for the maximum could be the Gibbs–Thomson effect that states that small crystals are more soluble than large ones. This phenomenon was established for $PbSO_4$ by Pavlov and Pashmakova [13]. When sufficient $PbSO_4$ nuclei are formed and reach a certain size, the lead-ion concentration diminishes until an equilibrium value is reached and maintained until the end of discharge.

According to Fig. 12, there are small, unoxidized $PbSO_4$ crystallites within the volume of PbO_2 agglomerates. The appearance of the maximum implies that these crystallites have practically no effect on the $PbSO_4$

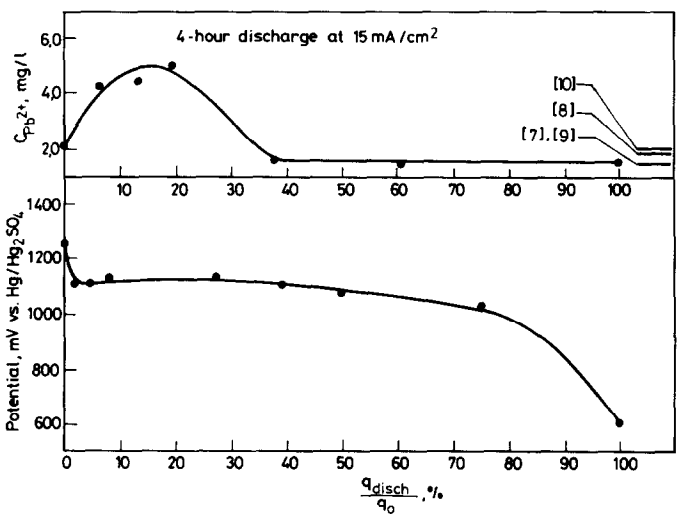

Fig. 13. Potential and concentration of soluble lead ions in active mass pores during discharge at 15 mA cm^{-2} for 4 h. Small lines on right-hand side correspond to solubility values given in Table 1. Potential *vs.* Hg/Hg_2SO_4 reference electrode.

TABLE 1

Solubility of $PbSO_4$ in H_2SO_4 (sp. gr. 1.28)

Authors	Pb^{2+} l^{-1} (mg)	Reference
1. Crockford and Brawly	1.5	7
2. Vinal and Craig	1.95	8
3. Danel and Plichon	1.5	9
4. Li *et al.*	2.1	10

nucleation rate which, in turn, may indicate that the crystals have no contact with the solution in the pores.

Charge

Figure 14 presents the change in potential and lead-ion concentration in the pores during charge under different conditions. Solubility data of lead

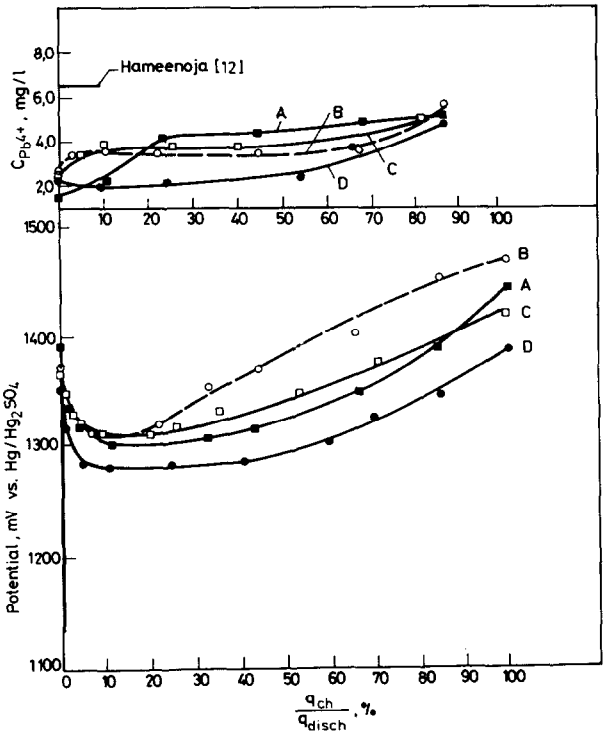

Fig. 14. Potential and concentration of lead ions (Pb^{2+}, Pb^{4+} and soluble lead compounds) in pores of active mass during charge. A, 5 h charge (13.3 mA cm^{-2}) after 4 h discharge (15 mA cm^{-2}); B, 5 h charge (13.3 mA cm^{-2}) after 4 h discharge (15 mA cm^{-2}) and 18 h rest period in H_2SO_4 solution; C, 5 h charge (13.3 mA cm^{-2}) after 20 h discharge (3.75 mA cm^{-2}); D, 10 h charge (7.0 mA cm^{-2}) after 20 h discharge (3.75 mA cm^{-2}). Measurements terminated after commencement of gas evolution.

dioxide are also given, as calculated by Hameenoja *et al.* [12] during $PbSO_4$ oxidation on a rotating disc electrode. The total amount of soluble lead was determined in this case (Pb^{2+}, Pb^{4+}, and soluble hydroxides). After a certain period of time, the lead-ion concentration increased and reached values between 3.5 and 4.5 mg l^{-1}. Given that Pb^{2+} ions are consumed in the reaction, it can be expected that during charge the tetravalent ions and complexes will prevail in the pores. The experimental values reported here for the soluble Pb^{4+} compounds are lower than those calculated by Hameenoja *et al.* [12].

The idea of the formation of tetravalent lead ions and complexes during battery charge has undergone certain developments in the literature. Feitknecht and Gaumann [14] were the first to assume that the $PbSO_4$ oxidation reaction to PbO_2 passes through soluble Pb^{4+} compounds $(Pb(OH)_2(SO_4)_2)^{2-}$ or $Pb(SO_4)_2$, which are unstable in H_2SO_4 and form PbO_2 by disproportionation. Vankova *et al.* [15] found that the solubility of commercial PbO_2 in H_2SO_4 is 38 mg l^{-1} and forms the soluble species $PbO(OH)_2$ and $PbO(OH)^+$. In rotating disc electrode studies, Skyllas-Kazacos [16, 17] demonstrated the formation of a soluble Pb^{4+} compound during the oxidation of Pb and $PbSO_4$. Using the same technique, Hameenoja *et al.* [12] determined the concentration of Pb^{4+} in the solution to be 6.4 mg l^{-1}.

Gas evolution commences on the plate when the state-of-charge reaches 60 - 70%; hence the concentration measurements were terminated in most cases. Several concentration values were determined under conditions of oxygen evolution. The values are very high and are due to an error introduced by gas evolution rather than to the actual conditions of the phenomenon. On the other hand, it is well known that the dissolution rate of PbO_2 increases at higher potentials and intensive gas evolution [18, 19]. Hence, the increase in the concentration of soluble tetravalent lead ions and complexes may be partially due to these phenomena.

Discussion

On the reversibility of crystallization processes during battery cycling

During discharge, considerable amounts of the PbO_2 agglomerates are partially, or fully, disintegrated through the formation of large $PbSO_4$ crystals (Figs. 2 - 4). The major part of the macrostructural level, however, remains intact and conducts the electric current during charge. During charge, the integrity of this level is restored either by metasomatic processes or by free formation of PbO_2 agglomerates. The latter consist of small PbO_2 particles separated by pores; these particles are formed from the large $PbSO_4$ crystals whose volume becomes the matrix of the PbO_2 agglomerates. The microstructure of these new agglomerates is organized in a manner similar to that of the remaining unoxidized part of the active mass after discharge. Hence, the structural elements of the active mass are rebuilt. This phenomenon ensures that the battery is able to withstand a large number of charge/discharge cycles.

The macrostructural level, on the other hand, alters with cycling. Depending on the size, shape, and mode of linkage of the $PbSO_4$ crystals, as well as on the proportion between the metasomatic processes and those of free formation during charge, PbO_2 agglomerates will differ in shape, size, and mode of inter-connection.

It is worth mentioning that $PbSO_4$ recrystallization takes place preferably in the large pores (Figs. 2, 3). During metasomatic oxidation of the recrystallized $PbSO_4$ particles, only slight hindrances are created to the ion transport during both charge and discharge. Hence, due to the nature of the recrystallization processes, polarization caused by transport hindrances of the ions is maintained at a low level.

On the other hand, it has been established that during charge not all the $PbSO_4$ crystals can be oxidized to PbO_2 (Figs. 7, 10, 12). Unoxidized $PbSO_4$ grains may remain in the PbO_2 agglomerates. This depends on the presence of impurities that may inhibit, or enhance, these processes. Thus, such impurities can serve as either useful or detrimental dopants in the positive active mass. When the $PbSO_4$ oxidation process is inhibited, continuous undercharging will occur and may result in capacity loss.

It has been shown [2] that during charge and discharge the active mass is pulsating. The formed $PbSO_4$ phase creates mechanical tensions in the PbO_2 skeleton and the plate thickness increases. During charge, these tensions are released and the plate shrinks. Its initial state cannot, however, be fully restored and the plate gradually swells. This leads to the formation of large pores in the PbO_2 active mass that, in turn, affect the crystallization processes. When the volume of these large pores exceeds a certain critical value, the bonds between the PbO_2 agglomerates are loosened and the active material is softened and begins to shed from the plate.

The above experimental results show that PbO_2 agglomerates are the basic building elements that reproduce the properties of the active mass as a whole. Their structure, rigidity, and microporosity determine the capability of the active mass for power generation and power accumulation. The individual PbO_2 particles and associated micropores represent the agglomerate components that have different properties and functions determined by the local conditions. Their statistical summation gives the agglomerate characteristics.

Elementary processes during positive plate charge

Based on the above observations and experimental data, the charging process can be represented by the scheme in Fig. 15. The different stages of this scheme are as follows.

$PbSO_4$ dissolution

A definite Pb^{2+} concentration is maintained at the surface of $PbSO_4$ crystals or/and in the bulk of the pore solution surrounding them. This concentration is equal to the solubility of $PbSO_4$ and is presented in Fig. 13 as determined at the end of discharge.

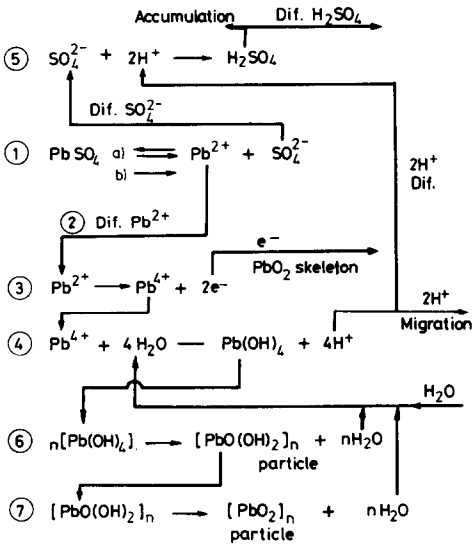

Fig. 15. Scheme for elementary processes during charging of positive active mass.

As can be seen from Figs. 6 - 9, some of the $PbSO_4$ crystals react rapidly to the changes in Pb^{2+} ion concentration, *e.g.*, during charge the crystals are rounded. This implies that they maintain a reversible Pb^{2+} concentration in the pores of the active mass. Other $PbSO_4$ crystals, however, preserve their apices and edges — even when strongly affected by the oxidation process. It can be assumed that they are partially passivated and that the exchange of Pb^{2+} with the pore solution is strongly inhibited. The concentration of Pb^{2+} ions in the pore volume (Fig. 13) is determined by the solubility of non-passivated $PbSO_4$ crystals.

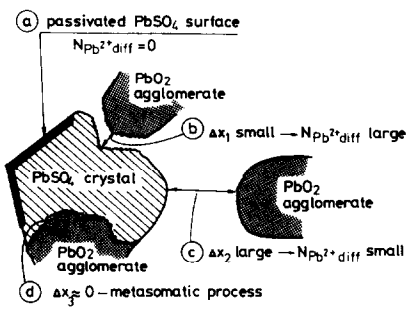

Fig. 16. Scheme for oxidation of a $PbSO_4$ crystal at different values of the diffusion path length (Δx) of Pb^{2+} ions.

Diffusion stage in Pb^{2+} ion transport

Lead ions (from the pore volume or the crystal surface) are transported by diffusion to the nearest PbO_2 agglomerate connected to the PbO_2 skeleton of the active mass.

The diffusion path length, Δx, of Pb^{2+} ions is defined by Fick's first law:

$$N_{\text{diff}}^{Pb^{2+}} = D_{Pb^{2+}}(\Delta C_{Pb^{2+}}/\Delta x) \tag{3}$$

Based on Figs. 6 - 10(a), a scheme of the various possibilities, as determined by the value of Δx, is presented in Fig. 16. It should be noted that the $PbSO_4$ crystal volume is much larger than the thickness of the reaction layer between the $PbSO_4$ surface and the PbO_2 agglomerate. When the $PbSO_4$ crystal surface is passivated, no dissolution takes place; hence no flow of Pb^{2+} ions occurs ((a), Fig. 16). When the $PbSO_4$ crystal is not passivated, three possible processes can be observed, namely, processes (b), (c) and (d), Fig. 16. If Δx is very small (process (b)), the flow of Pb^{2+} ions is intensive and the PbO_2 agglomerate may grow to dimensions similar to those of the oxidized $PbSO_4$ crystal. If Δx is very large (process (c)), the flow of Pb^{2+} ions is weak and the PbO_2 agglomerate "fails to remember" the size and form of the host $PbSO_4$ crystal. If $\Delta x \approx 0$ (process (d)), a metasomatic process takes place and the PbO_2 agglomerate repeats the shape and size of the $PbSO_4$ crystal.

Electrochemical reaction

Processes (3) and (4) in Fig. 15 occur in the strongly hydrated surface layer of the PbO_2 particle, and are consequently very complex. Most probably, the oxidation of Pb^{2+} ions proceeds in two stages. Part of the $PbSO_4$ crystals dissolve and disappear, while at the same time another solid phase, PbO_2, appears and starts to grow. A reaction layer is set up between the two phases where the processes are taking place. In most cases, the $PbSO_4$ crystal size may be many times larger than the thickness of the reaction layer. Hence, different parts of the $PbSO_4$ crystal can be oxidized at different rates.

Electroneutralization stage

Hydrogen ions are evolved during reaction (4) and SO_4^{2-} ions remain from reaction (1), Fig. 15. The electrical charges on these ions are not compensated. Flows of H^+ and HSO_4^- ions are formed between the reaction layer and the bulk of the solution; these flows maintain the electroneutrality of the solution in the reaction layer. The H_2SO_4 is mainly dissociated into H^+ and HSO_4^- ions (90 - 95%) at 1 - 5 M H_2SO_4. Thus, three H^+ and one HSO_4^- ions are formed for every $2e^-$. The ionic current is carried by $2t_1$ H^+ in an outward direction, and by $2(1-t_1)$ HSO_4^- in an inward direction through diffusion and migration of the above ions (t_1 is the transference number). Thus, there is a net production of $(3-2t_1)$ H_2SO_4 per $2e^-$ (reaction (5)). Part of it diffuses out of the plate and the rest accumulates in the pores. If the

transport of H^+ and HSO_4^- ions is strongly impeded, the solution in the reaction layer will be charged positively and the rate of the electrochemical reaction, (3), will be decreased, since this reaction generates positive charges. In many cases, the transport of H^+ and HSO_4^- ions could become the rate-determining process during charging of the plate.

Crystallization stage and formation of PbO_2 particles

This stage includes reactions (6) and (7), Fig. 15. A certain number of $Pb(OH)_4$ molecules come close together and form a cloud that is dehydrated, whereupon a new PbO_2 particle is nucleated or an existing one grows. This process has been established [20] by transmission electron microscope studies. Dehydration can proceed in successive stages in various parts of the PbO_2 particle. It has been established that the PbO_2 particle is composed of crystalline, amorphous and hydrated zones [20], and is an open system interacting rapidly with the solution in the pores [20]. It appears likely that at both the $Pb(OH)_4$ formation and crystallization stages, part of the tetravalent hydroxide is dissolved in the pore solution. The results in Fig. 14 present the concentration of such species. With the progress of the oxidation process, many PbO_2 particles are gathered into agglomerates.

The rates of the above elementary processes might be different, thus any one of them could become rate determining and its influence could determine the regions of oxidation in the $PbSO_4$ crystal.

Acknowledgements

The authors are grateful to N. Lange of the Royal Institute of Technology, Stockholm and to M. Iosifova of the Institute of Physical Chemistry, Bulgarian Academy of Sciences, for preparation of the scanning electron micrographs.

References

1 D. Pavlov and E. Bashtavelova, *J. Electrochem. Soc.*, *131* (1984) 1468.
2 D. Pavlov and E. Bashtavelova, *J. Electrochem. Soc.*, *133* (1986) 241.
3 J. Burbank, *J. Electrochem. Soc.*, *111* (1964) 765; *113* (1966) 10.
4 A. Simon and S. Caulder, *J. Electrochem. Soc.*, *117* (1970) 8, 987.
5 P. Ekdunge and D. Simonsson, *J. Electrochem. Soc.*, *132* (1985) 2521.
6 Z. Takehara and K. Kanamura, *J. Electrochem. Soc.*, *134* (1987) 13, 1604.
7 H. D. Crockford and D. J. Brawley, *J. Am. Chem. Soc.*, *56* (1934) 2600.
8 G. W. Vinal and D. N. Craig, *J. Res. Natl. Bur. Stand.*, *22* (1939) 55.
9 V. Danel and V. Plichon, *Electrochim. Acta*, *27* (1982) 771.
10 L. J. Li, M. Fleishmann and L. M. Peter, *Electrochim. Acta*, *32* (1987) 1585.
11 Z. Takehara and K. Kanamura, *Electrochim. Acta*, *29* (1984) 1643.
12 E. Hameenoja, T. Laitinen and G. Sundholm, *Electrochim. Acta*, *32* (1987) 187.
13 D. Pavlov and I. Pashmakova, *J. Appl. Electrochem.*, *17* (1987) 1075.

14 W. Feitknecht and A. Gaumann, *J. Chim. Phys.*, *49* (1952) 135.
15 L. V. Vanjukova, M. M. Isaeva and B. N. Kabanov, *Dokl. Akad. Nauk SSSR*, *142* (1962) 377.
16 M. Skyllas-Kazacos, *J. Power Sources*, *13* (1984) 55.
17 M. Skyllas-Kazacos, *J. Electrochem. Soc.*, *128* (1981) 817.
18 P. C. Foller and C. W. Tobias, *J. Electrochem. Soc.*, *129* (1982) 506.
19 J. C. G. Thanos and D. W. Wabner, *J. Electroanal. Chem.*, *182* (1985) 25, 37.
20 D. Pavlov, I. Balkanov, T. Halachev and P. Rachev, *J. Electrochem. Soc.*, *136* (1989) 3189.